

3D Spectromicroscopic Observation of Yb-Silicate Ceramics Using XAFS-CT

Yasuo Takeichi^{1,*}, Toshiki Watanabe¹, Yasuhiro Niwa¹, Satoshi Kitaoka² and Masao Kimura¹

¹ Institute of Materials Structure Science, High Energy Accelerator Research Organization (KEK), Tsukuba, Japan.

² Japan Fine Ceramics Center, Nagoya, Japan.

* Corresponding author, yasuo.takeichi@kek.jp

Environmental barrier coatings (EBCs) are known to play an important role in enhancing the operating temperatures of gas-turbine engines [1]. A coating material in an operating engine undergoes various chemical reactions caused by oxygen, water vapor and other chemicals in the high-temperature combustion exhausts. Therefore, investigation of the chemical properties in the nanoscales is important to understand the degradation of EBCs. Here we report a result showing the 3D distribution of the chemical properties of ytterbium silicates (Yb–Si–O) [2], a candidate for top-coat materials of next generation EBCs.

Ytterbium disilicate (Yb₂Si₂O₇) ceramics is reported to contain precipitates of Yb₂SiO₅, and the transition between Yb₂Si₂O₇ and Yb₂SiO₅ is suggested to result from the chemical reactions during formation and operation [2]. Since ytterbiums in both silicates are Yb³⁺ surrounded by O²⁻ ions, Yb L₃-edge absorption spectra were only slightly different from each other. Therefore, this system would be a good test case to evaluate the spectroscopic capability of an X-ray microscope other than its importance as coatings; factors such as illumination homogeneity and stability, linearity of the detector, accuracy of the alignment and reconstruction, may affect the absorption spectra extracted from the 3D dataset.

A XAFS-CT instrument, an X-ray microscope combined with X-ray absorption fine structure, was recently installed at PF-AR NW2A beamline in KEK, Japan. The microscope (Xradia Ultra, Carl-Zeiss X-ray Microscopy, Inc.) was designed to work at the photon energy range of 5–11 keV. The illumination through the condenser capillary is homogenized using the agitators. The zone plate and optical magnification allows the projections of 20–40 μm FOV on the 12-bit 2k×2k CCD detector. The spatial resolution was confirmed to be <30 nm in the 2D observation. The magnification is maintained constant by moving the detector position along the X-ray beam axis depending on the photon energy.

The Yb–Si–O sample material was prepared as a sintered wafer by ultrasonic spray pyrolysis method [2]. The wafer was crushed to pick up a particle of 10–20 μm diameter for XAFS-CT observation. Projection images were obtained using a zone plate with the diameter and outermost zone width of 100 μm and 30 nm, respectively. Each of the tomographies with 361 projections was repeated at 36 energy points in a range of 8900–9060 eV (around Yb L₃-edge). Total acquisition time was about 12 hours. Alignment and reconstruction at each photon energy were performed using TXM Wizard software [3]. The voxel size was 24.4 nm for reconstruction, but was binned to 48.8 nm for segmentation described below.

The rendered 3D structure of Yb–Si–O sample observed at 8980 eV is shown in Fig. 1(a). It was difficult to distinguish Yb₂Si₂O₇ and Yb₂SiO₅ only using raw spectrum of each voxels, though island/sea structures with micropores were clearly observed in the 3D images. Therefore, we segmented the 3D images into high-density island and low-density sea regions. Morphological Segmentation plugin [4] of Fiji software package was used to segment the data. This plugin allows labeling and segmentation by the

watershed analysis of the gradient of the absorption intensity. Figure 1(b) shows a slice of the segmented 3D image at the dotted line in Fig. 1(a). The segmentation successfully exploited grain/porous structures, while omitting the local fluctuations of the X-ray absorption possibly due to the projection and/or reconstruction artifacts.

Fig. 2 shows the averaged absorption spectra of the high-density island and low-density sea regions. Spectrum of each region was fitted by the linear combination of standard spectra, $\text{Yb}_2\text{Si}_2\text{O}_7$, Yb_2SiO_5 , and Yb_2O_3 . The fitting range was limited to 8954–9040 eV because the intensities at the white-line peak at around 8946 eV showed some deviation, possibly due to large absorption. However, as shown in the inset of Fig. 2, a slight but significant difference in the fitting range quantified the fraction of the three standards. The high-density island region was found to contain >70% of Yb_2SiO_5 , while the low-density sea region was pure (>99%) $\text{Yb}_2\text{Si}_2\text{O}_7$. The amount of Yb_2O_3 was found to be negligible for both spectra. From this result we concluded that, from the spectroscopic point of view, the chemical state of Yb in island grains was identical to that of Yb_2SiO_5 .

Moreover, these results tell that XAFS-CT observation is useful for evaluating not only the edge energy or valency, but also detailed X-ray absorption structures in the post-edge area. On the other hand, they have also shown the difficulty in obtaining a correct absorption spectrum, especially for materials whose spectrum has a sharp white-line peak, where the high linearity of the detector is required to cover a whole energy range of the absorption spectra [5].

References:

- [1] D R Clarke and C G Levi, *Annu. Rev. Mater.* **33** (2003), 383.
- [2] M Wada *et al.*, *Acta Mater.* **135** (2017) 372.
- [3] Y Liu *et al.*, *J. Synchrotron Rad.* **19** (2012), 281.
- [4] D Legland *et al.*, *Bioinformatics* **32** (2016), 3532.
- [5] This work was supported by the Structural Materials for Innovation of the Cross ministerial Strategic Innovation Promotion Program (SM⁴I, SIP) of Japan Science and Technology (JST). Experiments were performed under the approval of the Photon Factory Program Advisory Committee (Proposal Nos. 2015S2-002 and 2016S2-001).

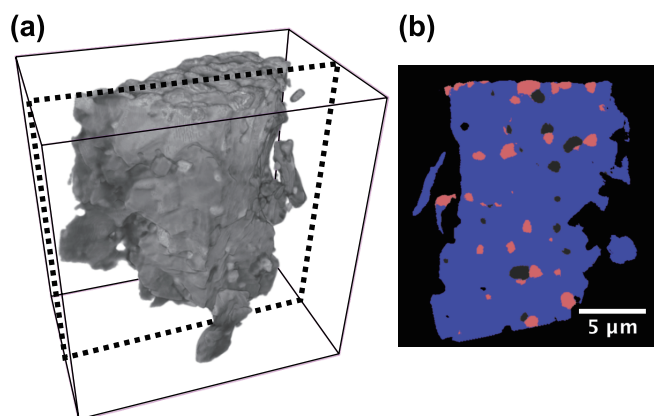


Figure 1. (a) 3D view of a reconstructed Yb–Si–O sample observed at 8980 eV. (b) A slice of segmented dataset at dotted lines drawn in (a).

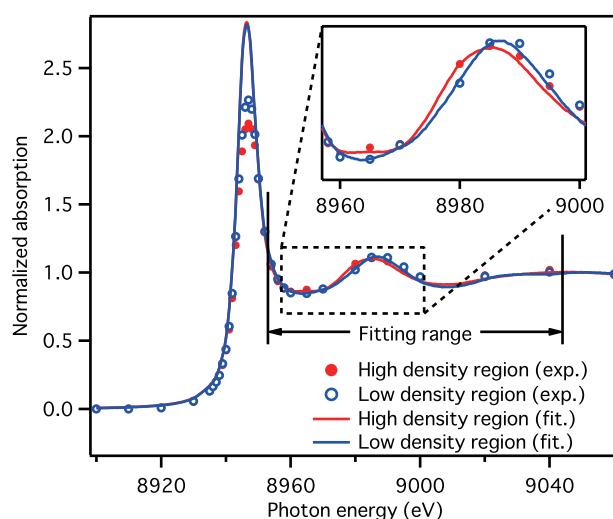


Figure 2. Yb L_3 -edge X-ray absorption spectra and fitting results of the red and blue regions shown in Fig. 1(b).